IEEE Access
Multidisciplinary | Rapid Review | Open Access Journal

Received January 17, 2020, accepted January 31, 2020, date of publication February 4, 2020, date of current version February 11, 2020.

Digital Object Identifier 10.1109/ACCESS.2020.2971505

A Gravitational Search Algorithm With Chaotic Neural Oscillators

YIRUI WANG[1], SHANGCE GAO[1], (Senior Member, IEEE), YANG YU[1], ZIQIAN WANG[1], JIUJUN CHENG[2], AND YUKI TODO[3]

[1]Faculty of Engineering, University of Toyama, Toyama 930-8555, Japan
[2]Key Laboratory of Embedded System and Service Computing, Department of Computer Science and Technology, Ministry of Education, Tongji University, Shanghai 200092, China
[3]Faculty of Electrical and Information and Computer Engineering, Kanazawa University, Kanazawa-shi 920-1192, Japan

Corresponding authors: Shangce Gao (gaosc@eng.u-toyama.ac.jp), Jiujun Cheng (chengjj@tongji.edu.cn), and Yuki Todo (yktodo@ec.t.kanazawa-u.ac.jp)

This work was supported in part by the JSPS KAKENHI under Grant JP19K12136, in part by the National Natural Science Foundation of China under Grant 11572084, Grant 11972115, and Grant 61872271, and in part by the Fundamental Research Funds for the Central Universities under Grant 22120190208.

ABSTRACT Gravitational search algorithm (GSA) inspired from physics emulates gravitational forces to guide particles' search. It has been successfully applied to diverse optimization problems. However, its search performance is limited by its inherent mechanism where gravitational constant plays an important role in gravitational forces among particles. To improve it, this paper uses chaotic neural oscillators to adjust its gravitational constant, named GSA-CNO. Chaotic neural oscillators can generate various chaotic states according to their parameter settings. Thus, we select four kinds of chaotic neural oscillators to form distinctive chaotic characteristics. Experimental results show that chaotic neural oscillators effectively tune the gravitational constant such that GSA-CNO has good performance and stability against four GSA variants on functions. Three real-world optimization problems demonstrate the promising practicality of GSA-CNO.

INDEX TERMS Chaotic neural oscillator, chaotic state, gravitational constant, gravitational search algorithm.

I. INTRODUCTION

Metaheuristic algorithms have been attracting more and more attention for addressing various optimization problems [1]–[3]. They possess novel search mechanisms without precise mathematical calculation to find global optimal solutions. Thus, they can resolve several complicated and difficult problems, such as multi-objective optimization [4], [5], dynamic optimization [6], [7], classification and prediction [8], [9]. Their successful applications have verified their good effectiveness and efficiency.

Metaheuristic algorithms can be classified into three categories: biology-based algorithms, physics-based algorithms and geography-based algorithms. Biology-based algorithms are inspired from natural evolution and biological behaviors, which consist of swarm-based algorithms and evolution-based algorithms. Swarm-based algorithms mimic cooperative behaviors of social nature, such as ant colony optimization (ACO) [10] and particle swarm optimization (PSO) [11]. A swarm consists of many distinctive individuals and shows global social behaviors without central control. Individuals in a swarm are relatively simple whereas their collaboration can exert remarkable effect to handle different missions. Evolution-based algorithms are inspired from biological evolution. Biological operators including natural selection, crossover and mutation are introduced into algorithms to improve their search abilities. Thus, these algorithms have learning, adaptive and evolutionary capabilities, such as genetic algorithm (GA) [12], evolutionary programming (EP) [13] and differential evolution (DE) [14]–[17]. Physics-based algorithms are designed from physical phenomenon and rules, such as simulated annealing (SA) [18] and GSA [19]. Geography-based algorithms are to search space according to geography, such as Tabu search (TS) [20] and imperialistic competition algorithm (ICA) [21]. These algorithms have two crucial properties, i.e., exploration and exploitation. Exploration means that algorithms sufficiently search an entire space without trapping into

The associate editor coordinating the review of this manuscript and approving it for publication was Chao Shen.

local optima. Exploitation indicates that algorithms further optimize the search space in order to find a better solution. To obtain better results, the balance between exploration and exploitation should be considered. Consequently, numerous researchers focus on them to improve performances of algorithms.

As a metaheuristic algorithm, GSA is proposed from the concept of gravity. It endows gravitational forces, masses, accelerations to particles. Particles emulate the law of gravity to implement their search. GSA has shown great potential in the field of optimization and engineering [22]. Its various variants have been devised from the perspective of operators. In [23], a disruption operator was proposed to improve the search ability of GSA. In [24], two mutation operators were used to alleviate the premature convergence of GSA. In [25], an orthogonal crossover operator was used to accelerate the convergence of GSA. In [26], a niching operator was proposed to enable GSA to find multiple solutions. In [27], chaotic operators were utilized to enhance the performance of GSA. Besides, Kepler operator [28], escaping operator [29] and repulsive operator [30] were introduced to optimize particles' positions. These operators effectively improve particles' movements.

In addition to operators, diverse strategies can also strengthen GSA. Self-adaptive strategies use adaptive methods to adjust current conditions of GSA. In [31], particles self-adaptively selected two updating methods to obtain optimal solutions. In [32], an adaptive alpha was calculated via particles' states and positions. In [33], hyperbolic functions were used to adaptively adjust acceleration coefficients, gravitational constant and several best particles. Chaotic strategies adopt chaotic ergodicity and stochasticity to optimize particles' search ranges. In [34], chaotic maps were used to adjust the gravitational constant. In [35], chaotic local search was employed to further exploit global optimal solutions. Hybrid strategies apply characteristics of several approaches to tackle the limitation of GSA. In [36], PSO was used to improve the search ability of GSA. In [37], dynamic multi-swarm PSO and GSA were hybridized to enhance the performance of algorithm. In [38], an opposition-based learning method was combined with GSA. In [39], quantum mechanics theories were applied to GSA to prevent its premature convergence. In [40], a hierarchical structure was embedded into GSA. An incremental social learning structure was also added into GSA for high-dimensional functions [41]. In [42], neural network and fuzzy system were used to adjust the alpha value of GSA. The alpha value was also tuned via a fuzzy controller optimized by GA, PSO and DE [43]. In [44], a quasi-Newton method was added into a chaotic GSA. These strategies help GSA overcome own disadvantages such that its performance is enhanced.

For different optimization problems, GSA variants have continuous, discrete and mixed types. Continuous type with real-valued variables can resolve real problems [19], [45], dynamic constrained problem [46], multi-modal and multi-objective problems [24], [26]. Discrete type with discrete values can address binary problem [47], graph planarization problem [48] and knapsack problem [49]. Mixed type can tackle problems with both continuous and discrete variables [50], [51]. Furthermore, GSA has been applied to many engineering problems such as design of type controllers [52], exergy efficiency of geothermal power plants [53], wind power system [54], Internet of Things [55] and image segmentation [56], [57]. These wide applications show the potential power of GSA.

Although GSA can successfully optimize various problems, its search ability is limited by its own mechanism. To improve its performance, we use four kinds of chaotic neural oscillators to tune its gravitational constant, respectively. Outputs of chaotic neural oscillators show distinctive chaotic states, which effectively controls changes of gravitational forces. Thus, particles' search abilities are notably enhanced. Four chaotic neural oscillators are firstly measured on twenty-nine CEC2017 benchmark functions to determine the best one for improving GSA. Then, our proposed method GSA-CNO compares with four GSA variants to further verify the effect of chaotic neural oscillators. Finally, we apply GSA-CNO to three real-world optimization problems to show its practicality.

The contributions of this paper can be summarized as follows: (1) We innovatively use chaotic neural oscillators to tune the gravitational constant such that GSA has significant improvement. (2) Various chaotic states of chaotic neural oscillators provide a novel transition between exploration and exploitation processes in GSA. (3) Experiments demonstrate that chaotic neural oscillators are more effective than chaotic maps for adjusting the gravitational constant. (4) Our proposed algorithm has practicality for some real-world optimization problems.

The rest of this paper is organized as follows. Section II introduces original GSA. Section III presents our proposed GSA-CNO. Section IV carries out several experiments to analyze the performance of GSA-CNO on functions and real-world optimization problems. Section V summarizes this paper and gives some future work.

II. GSA

As a physics-based algorithm, GSA emulates the law of gravity to achieve mutual attraction among particles. High-mass particles attract low-mass ones to move towards them according to their gravitational forces. This principle effectively guides particles' search and movement. Good particles have high masses and appropriate positions such that the others can be attracted. Optimal solutions are gradually improved by particles' movement with iterations.

In GSA, a population has N particles. Each particle is expressed as $X_i = (x_i^1, \ldots, x_i^d, \ldots, x_i^D)$, $i \in \{1, 2, \ldots, N\}$ where D is dimension. Gravitational force $F_{ij}^d(t)$ between two particles X_i and X_j is described as

$$F_{ij}^d(t) = G(t)\frac{M_i(t) \times M_j(t)}{R_{ij}(t) + \varepsilon}(x_j^d(t) - x_i^d(t)) \tag{1}$$

where $G(t)$ is a gravitational constant. $M_i(t)$ and $M_j(t)$ are two particles' masses. $R_{ij}(t)$ is the Euclidean distance between them and ε is a small constant. The gravitational constant $G(t)$ is defined as

$$G(t) = G_0 \times e^{-\alpha \frac{t}{T}} \tag{2}$$

where G_0 is an initial value and α is a coefficient. T is maximum iteration count. Each particle's mass $M_i(t)$ is expressed as

$$m_i(t) = \frac{f_i(t) - f_w(t)}{f_b(t) - f_w(t)} \tag{3}$$

$$M_i(t) = \frac{m_i(t)}{\sum_{l=1}^{N} m_l(t)} \tag{4}$$

where $f_i(t)$ is fitness value. $f_w(t)$ and $f_b(t)$ are the worst and best fitness values, respectively. Since each particle X_i is attracted by others, its overall gravitational force $F_i^d(t)$ is obtained as

$$F_i^d(t) = \sum_{j \in K_{best}, j \neq i} rand_j \cdot F_{ij}^d(t) \tag{5}$$

where $rand_j$ is a random value in the interval (0,1). K_{best} indicates the first K best particles and K is linearly decreased with iteration t. Thereafter, each particle's acceleration $a_i^d(t)$, velocity $v_i^d(t+1)$ and position $x_i^d(t+1)$ are calculated as

$$a_i^d(t) = \frac{F_i^d(t)}{M_i(t)} \tag{6}$$

$$v_i^d(t+1) = rand_i \cdot v_i^d(t) + a_i^d(t) \tag{7}$$

$$x_i^d(t+1) = x_i^d(t) + v_i^d(t+1) \tag{8}$$

where $rand_i$ is a random value in the interval (0,1).

III. PROPOSED GSA-CNO

A. CHAOTIC NEURAL OSCILLATORS

Artificial neural networks use simple artificial neurons to simulate neural behaviors. Researchers have found that chaotic neural behaviors can be generated between excitatory and inhibitory neurons [58]. Thus, various chaotic neural models are proposed, such as chaotic oscillators [59], [60] and chaotic neural networks [61], [62]. These models can be applied to many complex problems such as pattern recognition and scene analysis [63], [64]. Chaotic neural oscillators show their powerful capabilities.

Recently, Lee-oscillator with retrograde signaling is a distinctive chaotic model [61]. It consists of four neurons, described as follows:

$$W(t) = tansig(I(t)) \tag{9}$$

$$L(t) = (V(t) - U(t)) \cdot e^{-kI^2(t)} + W(t) \tag{10}$$

$$U(t+1) = tansig(a_1 \cdot L(t) + a_2 \cdot U(t) - a_3 \cdot V(t) + a_4 \cdot I(t) - \theta_u) \tag{11}$$

$$V(t+1) = tansig(b_1 \cdot L(t) - b_2 \cdot U(t) - b_3 \cdot V(t) + b_4 \cdot I(t) - \theta_v) \tag{12}$$

$$tansig(t) = \frac{1 - e^{-2t}}{1 + e^{-2t}} \tag{13}$$

where $W(t)$, $L(t)$, $U(t)$ and $V(t)$ indicate input, output, excitatory and inhibitory neurons, respectively. k is a coefficient. a_i and b_i are weights of corresponding neurons. θ_u and θ_v are thresholds of excitatory and inhibitory neurons. $I(t) \in [-1, 1]$ is an input signal and $tansig(t)$ denotes a hyperbolic tangent sigmoid function.

Compared with other oscillators, Lee-oscillator with retrograde signaling has more chaotic states owing to its various parameter settings. Chaotic shapes and regions can be obtained by tuning parameters. A wide chaotic region can more effectively process intermediate information. Meanwhile, the number of iterations that a chaotic region needs is small such that its computational time is low. Based on these characteristics, Lee-oscillator with retrograde signaling can show a transient-chaotic attribute for temporal information processing.

B. GSA-CNO

Although GSA is an effective algorithm for many problems, it has low search ability and premature convergence. GSA uses gravitational forces among particles to guide the search direction of population. Thus, their gravitational forces play a crucial role in the search process. However, a gravitational constant considerably influences the gravitational force. More specifically, a great value of gravitational constant means a large gravitational force, which can lead to a large search range of particle. In other words, its search ability is improved. GSA adopts an exponential gravitational constant to control the gravitational force. In fact, it cannot guarantee sufficient exploration ability of particles owing to its fast decay. Meanwhile, exploitation ability of particles is also declined. Hence, premature convergence is prone to occur.

To address these disadvantages, we apply chaotic neural oscillators to adjust the gravitational constant. Based on Lee-oscillator with retrograde signaling, a normalization method is used to modify it as

$$Z(t) = \frac{d - c}{b - a} \times (L(t) - a) + c \tag{14}$$

where a and c indicate lower bounds of two intervals. b and d denote upper bounds of two intervals. Values of $L(t)$ are mostly in the interval $[-1, 1]$. Eq. (14) can map them into other intervals. In this paper, we set $a = -1$, $b = 1$, $c = 1$ and $d = 0$ to obtain values of $Z(t)$. New gravitational constant is calculated as

$$G(t) = G_0 \times Z(t) \tag{15}$$

According to different parameter settings of Lee-oscillator with retrograde signaling [61], we adopt four kinds of chaotic neural oscillators, i.e., CNO1, CNO2, CNO3 and CNO4, to control the gravitational constant, respectively. Their parameter settings are listed in Table 1. Their graphs are plotted in Fig. 1. It should be noted that iteration t is equivalent to the input signal $I(t)$ via normalization. From Fig. 1, four chaotic neural oscillators show different chaotic

TABLE 1. Parameter settings of four chaotic neural oscillators.

Parameter	CNO1	CNO2	CNO3	CNO4
a_1	0.90	0.50	-0.50	5
a_2	0.90	0.55	0.55	5
a_3	0.90	0.55	0.55	5
a_4	0.90	0.50	0.50	5
θ_u	0	0	0	0
b_1	-0.90	0.50	-0.50	-1
b_2	-0.90	-0.55	-0.55	-1
b_3	-0.90	-0.55	-0.55	-1
b_4	-0.90	-0.50	0.50	-1
θ_v	0	0	0	0
k	50	50	50	300

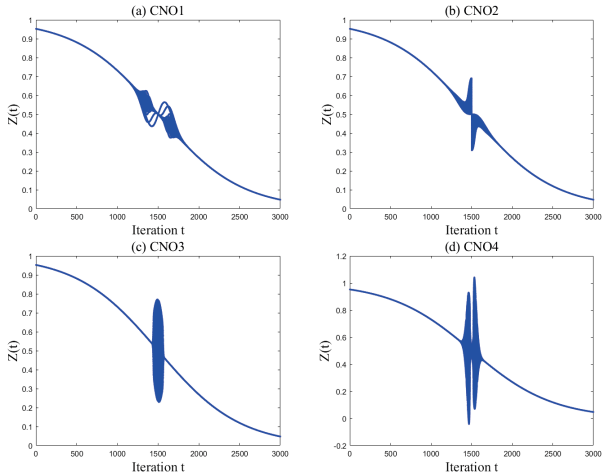

FIGURE 1. Graphs of four chaotic neural oscillators over 3000 iterations.

states over 3000 iterations. Moreover, they only generate chaos in intermediate regions. Fig. 2 displays their chaotic states in detail. From the viewpoint of time, CNO1 has a long chaotic period whereas CNO3 has a short one. From the viewpoint of change, CNO4 has a big chaotic amplitude whereas CNO1 has a small one. These four oscillators use own characteristics to tune the gravitational constant in order to improve the performance of GSA. Therefore, GSA-CNO is formed. Its pseudocode is given in Algorithm 1.

Compared with GSA, GSA-CNO uses chaotic neural oscillators to tune the gravitational constant such that its search ability is significantly improved. To be specific, an exponential gravitational constant in GSA decays quickly. Thus, GSA has insufficient time to explore an entire search space due to its small gravitational force. Furthermore, in a late search process, this exponential gravitational constant approximates zero. It cannot provide effective support for exploitation ability of GSA. However, for GSA-CNO, chaotic neural oscillators can maintain a great value of gravitational constant in a long period. It means that particles have large gravitational forces and sufficient time to search more regions. Hence, the exploration ability of algorithm is strengthened. In a late search process, chaotic neural oscillators still generate effective values to enable gravitational forces to guide particles. Accordingly, the exploitation ability of algorithm is

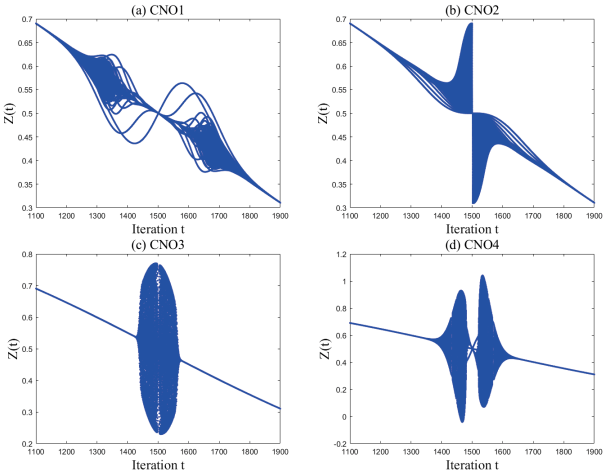

FIGURE 2. Chaotic states of four chaotic neural oscillators in intermediate regions.

Algorithm 1 GSA-CNO

Input: Parameters N, D, G_0, T, $a_1 - a_4$, θ_u, $b_1 - b_4$, θ_v, k

Output: Optimal solution

Initialization: Randomly generate N initial particles;
while *Termination criterion is not satisfied* **do**
  for $i = 1$ *to* N **do**
    if *Particle* X_i *is beyond the boundary* **then**
      Randomly reinitialize overstepping positions of particle X_i;
  for $i = 1$ *to* N **do**
    Evaluate the fitness $f_i(t)$ of particle X_i ;
  for $i = 1$ *to* N **do**
    Calculate the mass $M_i(t)$ of particle X_i according to Eqs. (3) and (4);
  Calculate the gravitational constant $G(t)$ according to Eqs. (9)-(15);
  Determine the K best particles as a set K_b ;
  for $i = 1$ *to* N **do**
    for $j = 1$ *to* K **do**
      Calculate the gravitational force between particle X_i and particle K_{b_j} according to Eqs. (1) and (5);
  for $i = 1$ *to* N **do**
    Update velocity and position of particle X_i according to Eqs. (6)-(8);
  $t = t + 1$;

also improved. Besides, chaotic neural oscillators have a distinctive attribute where chaos is generated in an intermediate search process. They use chaotic states to innovatively provide a period of transition between exploration and exploitation processes. Based on these differences, GSA-CNO

TABLE 2. Experimental and statistical results of GSA with four chaotic neural oscillators on twenty-nine CEC2017 benchmark functions with 30 dimensions.

Algorithm	F1	F2	F3	F4	F5	F6
GSA-CNO1	**3.08E+03 ± 1.52E+03**	6.12E+03 ± 1.98E+03	1.18E+02 ± 2.23E+00	1.76E+02 ± 1.15E+01	2.24E+01 ± 5.83E+00	**4.16E+01 ± 2.65E+00**
GSA-CNO2	3.08E+03 ± 1.65E+03 ∼	6.15E+03 ± 1.77E+03 ∼	**1.18E+02 ± 2.08E+00** ∼	**1.76E+02 ± 1.13E+01** ∼	**2.16E+01 ± 6.20E+00** ∼	4.24E+01 ± 3.14E+00 ∼
GSA-CNO3	3.77E+03 ± 1.90E+03 ∼	5.87E+03 ± 2.14E+03 ∼	1.19E+02 ± 2.41E+00 ∼	1.76E+02 ± 1.73E+01 ∼	2.36E+01 ± 7.14E+00 ∼	4.21E+01 ± 3.34E+00 ∼
GSA-CNO4	3.11E+03 ± 1.38E+03 ∼	**5.47E+03 ± 2.12E+03** ∼	1.18E+02 ± 2.48E+00 ∼	1.82E+02 ± 1.42E+01 ∼	2.27E+01 ± 5.20E+00 ∼	4.23E+01 ± 2.51E+00 ∼
	F7	F8	F9	F10	F11	F12
GSA-CNO1	1.19E+02 ± 1.38E+01	7.24E-04 ± 1.15E-04	**3.30E+03 ± 4.04E+02**	9.45E+01 ± 2.97E+01	**1.12E+04 ± 4.00E+03**	1.28E+04 ± 4.14E+03
GSA-CNO2	**1.18E+02 ± 1.37E+01** ∼	**7.17E-04 ± 1.67E-04** ∼	3.31E+03 ± 4.10E+02 ∼	9.46E+01 ± 2.97E+01 ∼	1.14E+04 ± 4.23E+03 ∼	1.28E+04 ± 4.05E+03 ∼
GSA-CNO3	1.19E+02 ± 1.27E+01 ∼	7.52E-04 ± 1.54E-04 ∼	3.44E+03 ± 4.38E+02 ∼	9.40E+01 ± 3.19E+01 ∼	1.21E+04 ± 4.97E+03 ∼	**1.25E+04 ± 4.93E+03** ∼
GSA-CNO4	1.19E+02 ± 8.63E+00 ∼	7.18E-04 ± 1.27E-04 ∼	3.61E+03 ± 4.72E+02 +	**8.86E+01 ± 2.62E+01** ∼	1.16E+04 ± 3.17E+03 ∼	1.36E+04 ± 4.50E+03 ∼
	F13	F14	F15	F16	F17	F18
GSA-CNO1	2.82E+03 ± 7.30E+02	7.80E+02 ± 5.32E+02	**1.24E+03 ± 2.43E+02**	**1.05E+03 ± 2.00E+02**	3.91E+04 ± 6.96E+03	3.25E+03 ± 1.36E+03
GSA-CNO2	**2.79E+03 ± 6.87E+02** ∼	**7.76E+02 ± 5.32E+02** ∼	1.24E+03 ± 2.43E+02 ∼	1.05E+03 ± 2.00E+02 ∼	**3.83E+04 ± 7.45E+03** ∼	3.25E+03 ± 1.36E+03 ∼
GSA-CNO3	2.88E+03 ± 1.19E+03 ∼	8.73E+02 ± 6.43E+02 ∼	1.25E+03 ± 2.08E+02 ∼	1.08E+03 ± 2.46E+02 ∼	4.46E+04 ± 1.06E+04 +	3.01E+03 ± 9.87E+02 ∼
GSA-CNO4	3.02E+03 ± 3.59E+03 −	8.58E+02 ± 5.62E+02 ∼	1.28E+03 ± 2.25E+02 ∼	1.10E+03 ± 1.92E+02 ∼	4.13E+04 ± 7.38E+03 ∼	**2.80E+03 ± 1.11E+03** ∼
	F19	F20	F21	F22	F23	F24
GSA-CNO1	8.58E+02 ± 1.82E+02	3.45E+02 ± 4.94E+01	6.86E+02 ± 1.52E+03	6.19E+02 ± 1.30E+02	**5.65E+02 ± 3.16E+01**	**3.87E+02 ± 2.90E+00**
GSA-CNO2	**8.57E+02 ± 1.86E+02** ∼	3.45E+02 ± 4.94E+01 ∼	6.92E+02 ± 1.53E+03 ∼	6.18E+02 ± 1.30E+02 ∼	5.65E+02 ± 3.16E+01 ∼	3.88E+02 ± 3.78E+00 ∼
GSA-CNO3	9.26E+02 ± 1.90E+02 ∼	**3.44E+02 ± 4.98E+01** ∼	8.39E+02 ± 1.68E+03 ∼	6.68E+02 ± 1.58E+02 ∼	5.66E+02 ± 2.19E+01 ∼	3.90E+02 ± 7.31E+00 ∼
GSA-CNO4	9.31E+02 ± 1.88E+02 +	3.57E+02 ± 1.74E+01 ∼	**4.07E+02 ± 1.17E+03** ∼	**6.10E+02 ± 1.30E+02** ∼	5.69E+02 ± 4.36E+01 ∼	3.90E+02 ± 7.70E+00 ∼
	F25	F26	F27	F28	F29	$w/t/l$
GSA-CNO1	2.64E+02 ± 4.87E+01	5.97E+02 ± 4.59E+01	**3.00E+02 ± 1.77E-03**	1.22E+03 ± 2.01E+02	4.62E+03 ± 8.76E+02	
GSA-CNO2	2.64E+02 ± 4.87E+01 ∼	5.96E+02 ± 4.55E+01 ∼	3.00E+02 ± 2.65E-03 +	1.22E+03 ± 2.04E+02 ∼	**4.62E+03 ± 5.77E+02** ∼	1/28/0
GSA-CNO3	**2.47E+02 ± 5.04E+01** ∼	**5.86E+02 ± 4.34E+01** −	3.00E+02 ± 2.78E-03 ∼	1.28E+03 ± 2.05E+02 ∼	4.99E+03 ± 9.13E+02 +	2/26/1
GSA-CNO4	2.57E+02 ± 5.01E+01 ∼	5.92E+02 ± 3.33E+01 ∼	3.00E+02 ± 2.20E-03 ∼	**1.16E+03 ± 1.73E+02** ∼	5.00E+03 ± 6.21E+02 +	3/25/1

effectively enhances its performance. In addition, GSA-CNO has the same computational time complexity $O(N^2)$ as GSA where N is population size. Thus, GSA-CNO is an effective and efficient algorithm.

C. CHARACTERISTICS OF GSA-CNO

GSA-CNO has three primary characteristics: (1) Its gravitational constant has continuity and discreteness. In a early or late search process, chaotic neural oscillators generate single values to adjust the gravitational constant, which shows its continuity. In an intermediate search process, chaotic gravitational constant exhibits its discreteness. (2) Its gravitational constant overall shows a sequentially decreasing process. Chaotic systems such as chaotic maps generally are unordered and random, but chaotic neural oscillators not only generates chaos but also maintains sequential changes of gravitational constant. (3) Chaotic gravitational constant offers the transition between exploration and exploitation processes. Chaos only improves the diversity of search behavior in the intermediate search process. It does not influence the exploration in a early search process and the exploitation in a late one. Thus, based on these three characteristics, GSA-CNO effectively controls its gravitational constant and reinforces its search ability.

IV. EXPERIMENTS

A. EXPERIMENTAL SETUP

Twenty-nine CEC2017 benchmark functions (F1-F29) are used to test performances of algorithms. F1-F2 are unimodal. F3-F9 are multimodal. F10-F19 are hybrid. F20-F29 are composition. Search space of functions is $[-100, 100]^D$ where D is dimension. Population size is 100. Initial gravitational constant G_0 is 100. Maximum number of function evaluations (NFEs) is $10000 * D$. Algorithms are run 30 times on each function. Experimental results are mean and standard deviation of optimization errors between obtained optimal solutions and known global ones. Their best values are highlighted in boldface. Statistical results are calculated by Wilcoxon rank-sum test at a significant level $\alpha = 0.05$. Wilcoxon rank-sum test is a nonparametric test for equality of population medians of two independent samples. It is equivalent to a Mann-Whitney U-test [65]. Its alternative hypothesis is that the distribution of one sample is smaller or greater than the other. U is the number of times where a y precedes an x in an ordered arrangement of elements in two independent samples X and Y, calculated as $U_X = R_X - \frac{n_X(n_X+1)}{2}$ and $U_Y = R_Y - \frac{n_Y(n_Y+1)}{2}$ where R_X and R_Y are the sum of ranks in two samples. n_X and n_Y are sizes of two samples. The smaller value between U_X and U_Y is used to consult significance tables. According to p-value, the significant difference between two samples can be obtained. In our statistical results, symbol + indicates that the main algorithm is better than the comparative one. Symbol − denotes the opposite situation. Symbol ∼ reveals that two algorithms have no significant difference. $w/t/l$ shows the number of win, tie and lose between two algorithms according to statistical results. All experiments are programmed by Matlab software on PC with 3.30GHz Intel(R) Core(TM) i5 CPU and 8GB RAM.

TABLE 3. Parameter settings of four GSA variants.

Algorithm	Parameters
GSA	$G_0 = 100, \alpha = 20$
CGSA	$G_0 = 100, \alpha = 20, MAX = 20, MIN = 1e^{-10}$, Sinusoidal map
PSOGSA	$G_0 = 100, \alpha = 20, w_1(t) = 0.5, w_2(t) = 1.5$
CGSA-M	$G_0 = 100, \alpha = 20, LP = 50$

B. COMPARISON FOR GSA-CNOS

We firstly evaluate four kinds of GSA-CNOs on twenty-nine CEC2017 benchmark functions with 30 dimensions. Experimental results in Table 2 show that they obtain the best mean on different functions, respectively. According to statistical results, GSA-CNO1 is slightly better than the others.

TABLE 4. Experimental and statistical results of five GSA variants on twenty-nine CEC2017 benchmark functions with 30 dimensions.

Algorithm	F1	F2	F3	F4	F5	F6
GSA-CNO1	3.08E+03 ± 1.52E+03	6.12E+03 ± 1.98E+03	**1.18E+02 ± 2.23E+00**	1.76E+02 ± 1.15E+01	**2.24E+01 ± 5.83E+00**	**4.16E+01 ± 2.65E+00**
GSA	1.90E+03 ± 1.03E+03 −	8.27E+04 ± 4.33E+03 +	1.42E+02 ± 1.59E+01 +	2.26E+02 ± 2.01E+01 +	5.02E+01 ± 2.75E+00 +	8.74E+01 ± 1.19E+01 +
CGSA	2.11E+03 ± 9.94E+02 −	1.70E+04 ± 1.85E+03 +	1.22E+02 ± 8.36E+00 +	2.11E+02 ± 2.08E+01 +	4.56E+01 ± 3.12E+00 +	5.13E+01 ± 5.87E+00 +
PSOGSA	4.02E+03 ± 3.26E+03 ∼	**3.26E+03 ± 7.87E+03** −	6.41E+02 ± 5.05E+02 +	**1.46E+02 ± 3.40E+01** −	2.44E+01 ± 8.94E+00 ∼	2.72E+02 ± 6.32E+01 +
CGSA-M	**1.72E+03 ± 7.79E+02** −	8.38E+04 ± 6.80E+03 +	1.36E+02 ± 1.95E+01 +	2.18E+02 ± 1.76E+01 +	5.14E+01 ± 4.18E+00 +	8.43E+01 ± 9.91E+00 +
	F7	F8	F9	F10	F11	F12
GSA-CNO1	**1.19E+02 ± 1.38E+01**	**7.24E-04 ± 1.15E-04**	**3.30E+03 ± 4.04E+02**	9.45E+01 ± 2.97E+01	**1.12E+04 ± 4.00E+03**	**1.28E+04 ± 4.14E+03**
GSA	1.51E+02 ± 1.31E+01 +	2.03E+03 ± 3.92E+02 +	3.87E+03 ± 4.34E+02 +	3.54E+02 ± 8.92E+01 +	1.03E+07 ± 1.93E+07 +	2.97E+04 ± 6.45E+03 +
CGSA	1.44E+02 ± 1.25E+01 +	9.07E+02 ± 2.68E+02 +	3.77E+03 ± 4.34E+02 +	**8.05E+01 ± 1.44E+01** ∼	1.26E+04 ± 2.80E+03 +	1.45E+04 ± 4.96E+03 ∼
PSOGSA	1.36E+02 ± 3.25E+01 +	3.64E+03 ± 1.67E+03 +	3.70E+03 ± 6.23E+02 +	3.87E+02 ± 3.14E+02 +	6.00E+07 ± 1.48E+08 +	2.39E+07 ± 7.46E+07 ∼
CGSA-M	1.52E+02 ± 7.97E+00 +	1.97E+03 ± 3.34E+02 +	3.94E+03 ± 4.11E+02 +	3.73E+02 ± 1.06E+02 +	1.46E+07 ± 2.66E+07 +	2.70E+04 ± 5.26E+03 +
	F13	F14	F15	F16	F17	F18
GSA-CNO1	**2.82E+03 ± 7.30E+02**	**7.80E+02 ± 5.32E+02**	**1.24E+03 ± 2.43E+02**	1.05E+03 ± 2.00E+02	**3.91E+04 ± 6.96E+03**	3.25E+03 ± 1.36E+03
GSA	4.72E+05 ± 1.31E+05 +	1.02E+04 ± 1.93E+03 +	1.58E+03 ± 2.84E+02 +	1.20E+03 ± 1.70E+02 +	3.18E+05 ± 1.76E+05 +	1.23E+04 ± 5.13E+03 +
CGSA	2.99E+03 ± 1.01E+03 ∼	9.26E+02 ± 7.05E+02 ∼	1.32E+03 ± 2.78E+02 ∼	1.14E+03 ± 2.06E+02 +	4.58E+04 ± 1.00E+04 +	**3.12E+03 ± 1.16E+03** ∼
PSOGSA	9.73E+04 ± 2.69E+05 ∼	5.29E+05 ± 2.82E+06 +	1.45E+03 ± 4.59E+02 +	**5.70E+02 ± 2.29E+02** −	3.05E+05 ± 1.01E+06 +	1.24E+04 ± 1.33E+04 +
CGSA-M	4.83E+05 ± 1.19E+05 +	1.00E+04 ± 1.93E+03 +	1.60E+03 ± 2.90E+02 +	1.13E+03 ± 1.92E+02 +	2.76E+05 ± 1.01E+05 +	1.15E+04 ± 4.79E+03 +
	F19	F20	F21	F22	F23	F24
GSA-CNO1	8.58E+02 ± 1.82E+02	3.45E+02 ± 4.94E+01	**6.86E+02 ± 1.52E+03**	**6.19E+02 ± 1.30E+02**	**5.65E+02 ± 3.16E+01**	**3.87E+02 ± 2.90E+00**
GSA	1.03E+03 ± 2.36E+02 +	4.57E+02 ± 1.95E+01 +	4.19E+03 ± 1.69E+03 +	1.26E+03 ± 1.23E+02 +	8.91E+02 ± 5.57E+01 +	4.32E+02 ± 1.22E+01 +
CGSA	1.03E+03 ± 2.13E+02 +	4.14E+02 ± 2.35E+01 +	2.66E+03 ± 2.31E+03 ∼	1.07E+03 ± 1.61E+02 +	7.58E+02 ± 4.32E+01 +	4.21E+02 ± 1.25E+01 +
PSOGSA	**5.74E+02 ± 2.35E+02** −	**3.29E+02 ± 3.53E+01** −	2.48E+03 ± 1.91E+03 +	6.33E+02 ± 8.75E+01 ∼	8.10E+02 ± 1.43E+02 +	5.20E+02 ± 7.53E+01 +
CGSA-M	1.01E+03 ± 1.88E+02 +	4.70E+02 ± 2.71E+01 +	3.69E+03 ± 2.08E+03 +	1.32E+03 ± 1.06E+02 +	8.85E+02 ± 5.28E+01 +	4.37E+02 ± 8.49E+00 +
	F25	F26	F27	F28	F29	$w/t/l$
GSA-CNO1	**2.64E+02 ± 4.87E+01**	**5.97E+02 ± 4.59E+01**	3.00E+02 ± 1.77E-03	**1.22E+03 ± 2.01E+02**	**4.62E+03 ± 8.76E+02**	
GSA	4.26E+03 ± 8.95E+02 +	1.97E+03 ± 3.21E+02 +	5.08E+02 ± 4.94E+01 +	1.81E+03 ± 2.10E+02 +	1.67E+05 ± 1.24E+05 +	28/0/1
CGSA	1.95E+03 ± 1.77E+03 ∼	1.25E+03 ± 2.27E+02 +	**3.00E+02 ± 4.90E-05** −	1.57E+03 ± 2.25E+02 +	1.29E+04 ± 1.44E+03 +	19/8/2
PSOGSA	3.10E+03 ± 1.30E+03 +	8.17E+02 ± 1.36E+02 +	7.16E+02 ± 2.00E+02 +	1.34E+03 ± 3.80E+02 +	3.39E+06 ± 1.42E+07 +	19/5/5
CGSA-M	4.13E+03 ± 6.61E+02 +	1.85E+03 ± 2.73E+02 +	5.22E+02 ± 4.92E+01 +	1.81E+03 ± 1.91E+02 +	1.64E+05 ± 9.29E+04 +	28/0/1

TABLE 5. Experimental and statistical results of five GSA variants on twenty-nine CEC2017 benchmark functions with 50 dimensions.

Algorithm	F1	F2	F3	F4	F5	F6
GSA-CNO1	1.52E+03 ± 2.48E+03	6.59E+04 ± 9.38E+03	1.87E+02 ± 5.81E+01	**2.77E+02 ± 1.74E+01**	**2.66E+01 ± 4.28E+00**	**7.34E+01 ± 3.88E+00**
GSA	7.71E+02 ± 8.68E+02 ∼	1.68E+05 ± 1.03E+04 +	1.99E+02 ± 6.18E+01 ∼	3.23E+02 ± 1.91E+01 +	5.72E+01 ± 3.03E+00 +	2.28E+02 ± 3.10E+01 +
CGSA	1.17E+03 ± 1.46E+03 ∼	5.82E+04 ± 4.23E+03 −	**1.35E+02 ± 8.40E+01** −	3.18E+02 ± 2.12E+01 +	5.29E+01 ± 3.47E+00 +	1.26E+02 ± 1.68E+01 +
PSOGSA	1.69E+09 ± 4.33E+09 +	**3.64E+04 ± 6.07E+04** −	3.30E+03 ± 2.22E+03 +	2.87E+02 ± 7.88E+01 ∼	3.48E+01 ± 7.66E+00 +	7.62E+02 ± 1.51E+02 +
CGSA-M	**7.62E+02 ± 1.06E+03** ∼	1.70E+05 ± 8.92E+03 +	2.23E+02 ± 6.62E+01 +	3.30E+02 ± 1.75E+01 +	5.67E+01 ± 2.47E+00 +	2.40E+02 ± 2.70E+01 +
	F7	F8	F9	F10	F11	F12
GSA-CNO1	3.04E+02 ± 1.90E+01	**5.04E+01 ± 2.34E+02**	**6.01E+03 ± 5.54E+02**	**1.25E+02 ± 1.34E+01**	**8.88E+04 ± 3.32E+04**	**5.87E+02 ± 6.62E+02**
GSA	3.55E+02 ± 2.15E+01 +	8.37E+03 ± 6.58E+02 +	6.98E+03 ± 6.19E+02 +	1.17E+03 ± 3.04E+02 +	1.92E+06 ± 5.40E+05 +	2.68E+04 ± 3.84E+03 +
CGSA	3.40E+02 ± 1.85E+01 +	6.24E+03 ± 5.36E+02 +	6.75E+03 ± 5.50E+02 +	1.32E+02 ± 7.27E+00 +	1.14E+05 ± 2.92E+04 +	5.04E+03 ± 7.53E+02 +
PSOGSA	**2.85E+02 ± 6.46E+01** ∼	1.17E+04 ± 3.13E+03 +	6.67E+03 ± 1.80E+03 ∼	4.10E+03 ± 4.61E+03 +	1.19E+09 ± 2.38E+09 +	2.36E+08 ± 7.44E+08 +
CGSA-M	3.61E+02 ± 1.79E+01 +	8.24E+03 ± 4.80E+02 +	6.72E+03 ± 5.77E+02 +	1.25E+03 ± 2.81E+02 +	1.76E+06 ± 3.88E+05 +	2.60E+04 ± 2.97E+03 +
	F13	F14	F15	F16	F17	F18
GSA-CNO1	1.51E+04 ± 4.72E+04	**7.62E+03 ± 1.85E+03**	**1.80E+03 ± 2.88E+02**	1.73E+03 ± 2.80E+02	**3.86E+04 ± 1.23E+04**	1.50E+04 ± 2.51E+03
GSA	2.98E+05 ± 1.14E+05 +	1.38E+04 ± 3.66E+03 +	2.13E+03 ± 3.60E+02 +	1.88E+03 ± 3.66E+02 +	1.38E+06 ± 8.69E+05 +	2.49E+04 ± 4.51E+03 +
CGSA	**1.24E+04 ± 1.28E+04** +	8.97E+03 ± 3.12E+03 +	1.85E+03 ± 2.82E+02 ∼	1.75E+03 ± 2.97E+02 ∼	4.15E+04 ± 1.01E+04 +	1.40E+04 ± 3.32E+03 ∼
PSOGSA	3.33E+06 ± 5.41E+06 +	2.14E+06 ± 1.09E+07 ∼	2.79E+03 ± 7.44E+02 +	**1.43E+03 ± 2.78E+02** −	1.14E+07 ± 1.42E+07 +	**1.02E+04 ± 1.06E+04** −
CGSA-M	3.59E+05 ± 4.18E+05 +	1.56E+04 ± 3.12E+03 +	2.04E+03 ± 3.67E+02 +	1.80E+03 ± 3.31E+02 ∼	1.35E+06 ± 8.39E+05 +	2.46E+04 ± 6.33E+03 +
	F19	F20	F21	F22	F23	F24
GSA-CNO1	**1.30E+03 ± 2.74E+02**	**4.68E+02 ± 2.88E+01**	8.20E+03 ± 4.06E+02	**1.02E+03 ± 1.81E+02**	**9.01E+02 ± 5.45E+01**	**5.76E+02 ± 2.82E+01**
GSA	1.61E+03 ± 2.84E+02 +	6.39E+02 ± 2.62E+01 +	9.10E+03 ± 5.11E+02 +	2.04E+03 ± 1.60E+02 +	1.36E+03 ± 6.39E+01 +	7.47E+02 ± 7.27E+01 +
CGSA	1.45E+03 ± 2.59E+02 +	5.91E+02 ± 3.01E+01 +	8.85E+03 ± 6.06E+02 +	1.73E+03 ± 1.48E+02 +	1.23E+03 ± 5.34E+01 +	6.63E+02 ± 3.97E+01 +
PSOGSA	1.32E+03 ± 4.38E+02 ∼	5.20E+02 ± 1.02E+02 +	**6.66E+03 ± 1.52E+03** −	1.23E+03 ± 2.19E+02 +	1.41E+03 ± 2.44E+02 +	2.25E+03 ± 1.06E+03 +
CGSA-M	1.48E+03 ± 2.79E+02 +	6.34E+02 ± 3.30E+01 +	9.18E+03 ± 4.45E+02 +	2.03E+03 ± 1.66E+02 +	1.36E+03 ± 7.09E+01 +	7.27E+02 ± 8.13E+01 +
	F25	F26	F27	F28	F29	$w/t/l$
GSA-CNO1	**3.00E+02 ± 2.63E-03**	**1.39E+03 ± 2.59E+02**	**5.03E+02 ± 1.90E+01**	**1.81E+03 ± 2.70E+02**	**1.26E+06 ± 1.20E+05**	
GSA	4.14E+03 ± 2.69E+03 +	3.68E+03 ± 3.58E+02 +	7.44E+02 ± 1.15E+02 +	2.67E+03 ± 4.38E+02 +	4.10E+07 ± 5.18E+06 +	27/2/0
CGSA	9.86E+02 ± 1.55E+03 −	2.90E+03 ± 3.09E+02 +	5.83E+02 ± 4.04E+01 +	2.14E+03 ± 2.89E+02 +	8.07E+06 ± 8.44E+05 +	22/4/3
PSOGSA	7.29E+03 ± 1.49E+03 +	2.01E+03 ± 4.32E+02 +	3.42E+03 ± 1.10E+03 +	3.26E+03 ± 1.22E+03 +	1.27E+08 ± 9.98E+07 +	20/5/4
CGSA-M	4.08E+03 ± 2.40E+03 +	3.77E+03 ± 4.87E+02 +	6.96E+02 ± 1.02E+02 +	2.67E+03 ± 4.12E+02 +	4.11E+07 ± 6.46E+06 +	27/2/0

The fact that four GSA-CNOs have similar results is expected because they only have different chaotic states in the intermediate search process. However, owing to their different chaotic states, GSA-CNO1 performs relatively better. It may be because chaos of CNO1 has a long period and small amplitudes to produce more effective gravitational forces. Thus, it can find better solutions on some functions. Despite these four GSA-CNOs overall improve their search performances and have similar results, we regard GSA-CNO1 as the best method.

C. COMPARISON FOR GSA VARIANTS

To further verify the performance of GSA-CNO1, four GSA variants including GSA [19], CGSA [34], PSOGSA [36] and CGSA-M [35] are adopted. Their comparisons are conducted on twenty-nine CEC2017 benchmark functions with 30 and 50 dimensions, respectively. Parameter settings of four GSA variants are listed in Table 3. Experimental results are shown in Tables 4 and 5.

In Table 4, GSA-CNO1 has the best mean on 20 functions. According to statistical results, GSA-CNO1 is significantly better than GSA, CGSA, PSOGSA and CGSA-M on 28, 19, 19 and 28 functions, respectively. It demonstrates that GSA-CNO1 has better performance on functions with 30 dimensions.

In Table 5, GSA-CNO1 obtains the best mean on 21 functions. $w/t/l$ manifests that GSA-CNO1 remarkably outperforms GSA, CGSA, PSOGSA and CGSA-M on 27,

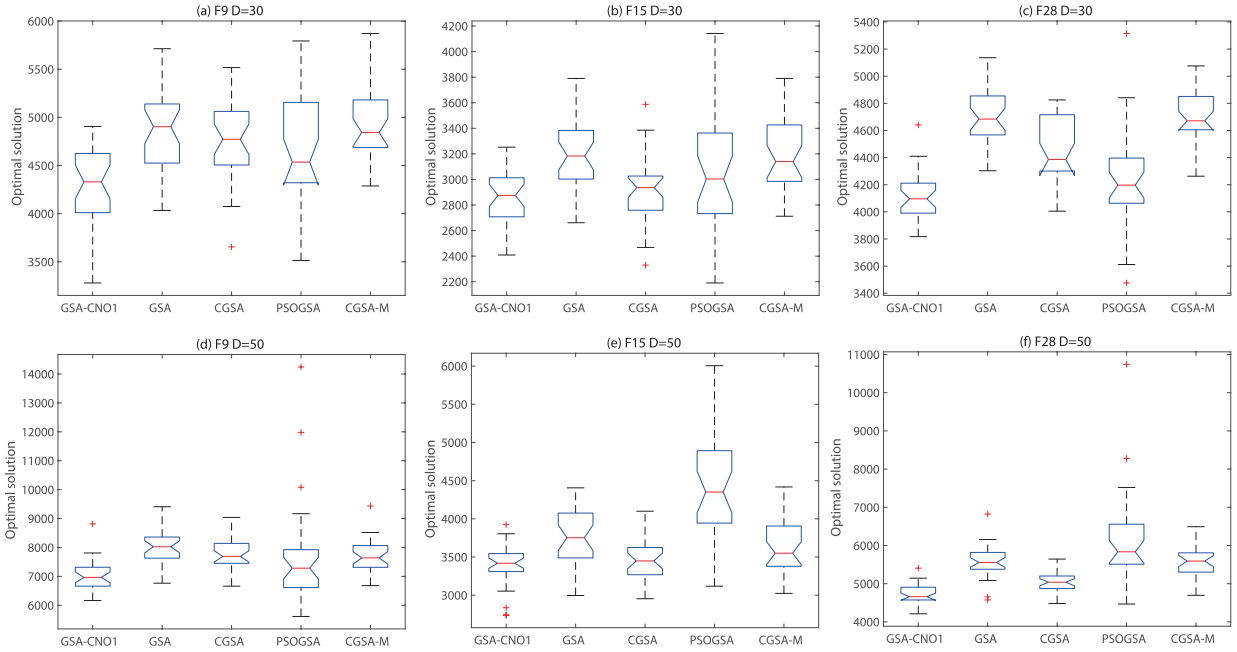

FIGURE 3. Box-and-whisker diagrams of optimal solutions obtained by five GSA variants on F9, F15 and F28 with 30 and 50 dimensions.

22, 20 and 27 functions, respectively. It still indicates the superiority of GSA-CNO1 on functions with 50 dimensions.

From Tables 4 and 5, we can give some remarks as follows: (1) The comparison between GSA-CNO1 and GSA verifies the effectiveness of chaotic neural oscillators for tuning gravitational constant. Chaotic neural oscillators are better than an exponential function to adjust gravitational forces. GSA-CNO1 significantly enhances its search performance. (2) The comparison between GSA-CNO1 and CGSA indicates that chaotic neural oscillators are better than chaotic maps. CGSA combines ten chaotic maps with gravitational constant to improve its performance where Sinusoidal map is the best [34]. However, GSA-CNO1 performs better than CGSA, suggesting that chaotic neural oscillators are more effective. (3) The comparison between GSA-CNO1 and PSOGSA denotes that the method of chaotic neural oscillators to control gravitational constant is superior to that of using global best individual to manage the population. (4) The comparison between GSA-CNO1 and CGSA-M illustrates that adjusting gravitational constant via chaotic neural oscillators outperforms using chaotic local search to improve the performance of GSA. The comparison among GSA-CNO1, PSOGSA and CGSA-M also reveals that adjusting the inherent property of GSA may be more reliable than employing external auxiliaries.

Fig. 3 plots box-and-whisker diagrams of optimal solutions obtained by five GSA variants on F9, F15 and F28 with 30 and 50 dimensions. Horizontal axis indicates five algorithms and vertical axis denotes values of optimal solutions. In Fig. 3, we can see that PSOGSA has the largest distribution of optimal solutions on three functions, implying that it is the most unstable. However, GSA-CNO1 has relatively small distribution of optimal solutions and its medians are smaller than other four GSA variants'. Thus, GSA-CNO1 has more stable and better performance.

Fig. 4 depicts convergence graphs of average fitness values obtained by five GSA variants on F8, F17 and F29 with 30 and 50 dimensions. Horizontal axis indicates NFEs and vertical axis denotes log value of average fitness. From Fig. 4, we can observe that GSA, PSOGSA and CGSA-M have premature convergence whereas GSA-CNO1 and CGSA show gradual convergence on three functions. It illustrates that adjusting gravitational constant can alleviate premature convergence. In addition, average fitness values of GSA-CNO1 are smaller than CGSA's, suggesting that chaotic neural oscillators are better than chaotic maps for tuning gravitational constant.

D. THREE REAL-WORLD OPTIMIZATION PROBLEMS

To verify the practicality of GSA-CNO1, three real-world optimization problems from CEC2011 are used. They are Lennard-Jones potential problem (LJPP), optimal control of a non-linear stirred tank reactor (OCNLSTR) and transmission network expansion planning problem (TNEPP). LJPP is the minimization of molecular potential energy with Lennard-Jones cluster. OCNLSTR is the optimal control of chemical reaction in a non-linear stirred tank reactor. TNEPP is to construct the set of transmission lines to minimize the cost of expansion plan and produce no overloads. Their specific descriptions and configurations can be referred in reference [66]. Five GSA variants are tested on these three problems. Experimental results are listed in Tables 6, 7 and 8 where Mean, Std, Best and Worst indicate mean value, standard deviation, minimum value and maximum value, respectively.

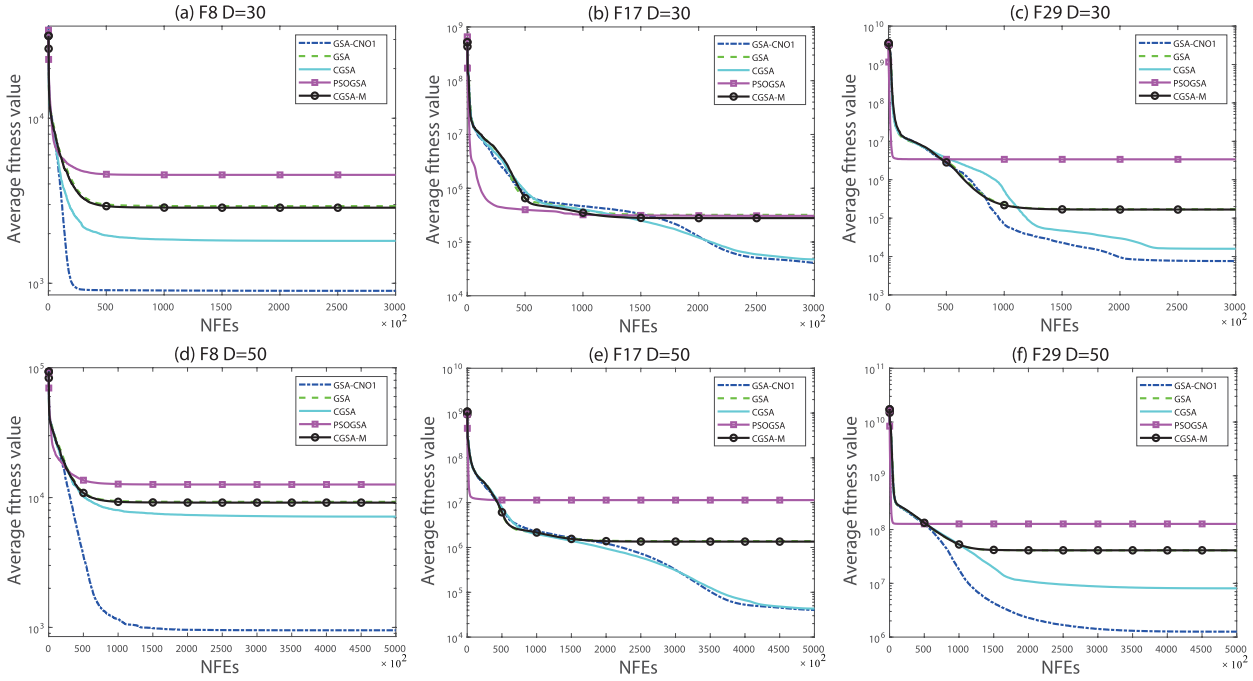

FIGURE 4. Convergence graphs of average fitness values obtained by five GSA variants on F8, F17 and F29 with 30 and 50 dimensions.

TABLE 6. Experimental results of five GSA variants on LJPP.

Algorithm	Mean	Std	Best	Worst
GSA-CNO1	-25.57	2.75	-28.37	-14.32
GSA	-16.97	4.06	-27.56	-10.03
CGSA	-24.93	2.71	-28.42	-18.53
PSOGSA	-24.58	2.70	-28.42	-19.16
CGSA-M	-18.60	3.17	-24.08	-11.23

TABLE 7. Experimental results of five GSA variants on OCNLSTR.

Algorithm	Mean	Std	Best	Worst
GSA-CNO1	15.57	1.88	14.00	20.89
GSA	21.55	0.73	20.58	24.32
CGSA	16.19	2.18	13.93	20.86
PSOGSA	21.45	1.54	14.33	23.88
CGSA-M	21.35	1.29	15.30	22.91

In Table 6, CGSA and PSOGSA obtain the minimum value −28.42 whereas GSA-CNO1 has the best mean value −25.57 on LJPP. It manifests that although CGSA and PSOGSA can find the best solution, GSA-CNO1 is more stable than them according to mean value. In Table 7, CGSA obtains the minimum value 13.93 and GSA-CNO1 has the best mean value 15.57 on OCNLSTR. It also shows good stability of GSA-CNO1. In Table 8, five algorithms find the minimum value 220 whereas GSA-CNO1 still has the best mean value 222.30. Meanwhile, standard deviation of GSA-CNO1 is far smaller than the others', which further highlights its effectiveness. These three real-world optimization problems reflect good stability and performance of GSA-CNO1 and demonstrate its promising practicality.

TABLE 8. Experimental results of five GSA variants on TNEPP.

Algorithm	Mean	Std	Best	Worst
GSA-CNO1	222.30	5.42	220	238
GSA	296.52	81.75	220	539.96
CGSA	260.12	40.49	220	350.55
PSOGSA	233.64	38.08	220	350.55
CGSA-M	269.37	55.33	220	445.19

V. CONCLUSION

A gravitational search algorithm with chaotic neural oscillators (GSA-CNO) is proposed to improve its search performance. Chaotic neural oscillators effectively adjust the gravitational constant to enhance gravitational forces among particles. Chaotic states provide a transition between exploration and exploitation processes. Thus, GSA-CNO significantly reinforces its property. Experiments verify superior performance of GSA-CNO against other GSA variants on functions and three real-world optimization problems. Besides, its computational time complexity is the same as original GSA. We can conclude that GSA-CNO is an effective and efficient algorithm.

This paper shows four valuable points. Firstly, we expand applications of chaotic neural oscillators on metaheuristic algorithms. To our knowledge, chaotic neural oscillators are firstly attempted to improve algorithms in this paper. Secondly, we illustrate that own parameters of GSA such as gravitational constant can considerably influence its performance. Compared with an original GSA, chaotic neural oscillators can better adjust the gravitational constant such that exploration and exploitation abilities of GSA are significantly enhanced. Thirdly, we provide a novel inspiration where

chaos can be used to be a transition between exploration and exploitation processes. Fourthly, we demonstrate that chaotic neural oscillators are more effective than chaotic maps for tuning the gravitational constant.

In the future work, several investigations could be considered as follows: (1) Gravitational constant could be controlled by other effective strategies to further improve the search performance of GSA. (2) Gravitational forces among particles could attempt to be enlarged by some interactive mechanisms to enhance particles' exploration and exploitation ability. (3) Chaotic neural oscillators could be added into other metaheuristic algorithms to diversify their search behaviors. (4) New GSA variants should be proposed to optimize complex engineering applications such as type controllers [67] and switched-mode power converters [68], [69].

REFERENCES

[1] Y. Yu, S. Gao, Y. Wang, Z. Lei, J. Cheng, and Y. Todo, "A multiple diversity-driven brain storm optimization algorithm with adaptive parameters," *IEEE Access*, vol. 7, pp. 126871–126888, 2019.
[2] T. Stützle and M. López-Ibáñez, "Automated design of metaheuristic algorithms," in *Handbook of Metaheuristics*. Cham, Switzerland: Springer, 2019, pp. 541–579.
[3] K. Hussain, M. N. M. Salleh, S. Cheng, and Y. Shi, "Metaheuristic research: A comprehensive survey," *Artif. Intell. Rev.*, vol. 52, no. 4, pp. 2191–2233, Dec. 2019.
[4] J. Wang, L. Yuan, Z. Zhang, S. Gao, Y. Sun, and Y. Zhou, "Multiobjective multiple neighborhood search algorithms for multiobjective fleet size and mix location-routing problem with time windows," *IEEE Trans. Syst., Man, Cybern., Syst.*, to be published, doi: 10.1109/tsmc.2019.2912194.
[5] J. Wang, B. Cen, S. Gao, Z. Zhang, and Y. Zhou, "Cooperative evolutionary framework with focused search for many-objective optimization," *IEEE Trans. Emerg. Topics Comput. Intell.*, to be published, doi: 10.1109/tetci.2018.2849380.
[6] S. Gao, Y. Wang, J. Cheng, Y. Inazumi, and Z. Tang, "Ant colony optimization with clustering for solving the dynamic location routing problem," *Appl. Math. Comput.*, vol. 285, pp. 149–173, Jul. 2016.
[7] Y. Wang, S. Gao, and Y. Todo, "Ant colony systems for optimization problems in dynamic environments," *Swarm Intell., Princ., Current Algorithms Methods*, vol. 119, pp. 85–120, Sep. 2018.
[8] S. Gao, M. Zhou, Y. Wang, J. Cheng, H. Yachi, and J. Wang, "Dendritic neuron model with effective learning algorithms for classification, approximation, and prediction," *IEEE Trans. Neural Netw. Learn. Syst.*, vol. 30, no. 2, pp. 601–614, Feb. 2019.
[9] Y. Wang, Y. Yu, S. Cao, X. Zhang, and S. Gao, "A review of applications of artificial intelligent algorithms in wind farms," *Artif. Intell. Rev.*, to be published, doi: 10.1007/s10462-019-09768-7.
[10] M. Dorigo and C. Blum, "Ant colony optimization theory: A survey," *Theor. Comput. Sci.*, vol. 344, nos. 2–3, pp. 243–278, Nov. 2005.
[11] R. Eberhart and J. Kennedy, "Particle swarm optimization," in *Proc. IEEE Int. Conf. Neural Netw.*, vol. 4, Nov. 1995, pp. 1942–1948.
[12] D. Weile and E. Michielssen, "Genetic algorithm optimization applied to electromagnetics: A review," *IEEE Trans. Antennas Propag.*, vol. 45, no. 3, pp. 343–353, Mar. 1997.
[13] X. Yao, Y. Liu, and G. Lin, "Evolutionary programming made faster," *IEEE Trans. Evol. Comput.*, vol. 3, no. 2, pp. 82–102, Jul. 1999.
[14] K. V. Price, "Differential evolution," in *Handbook of Optimization*. Berlin, Germany: Springer, 2013, pp. 187–214.
[15] S. Gao, Y. Wang, J. Wang, and J. Cheng, "Understanding differential evolution: A Poisson law derived from population interaction network," *J. Comput. Sci.*, vol. 21, pp. 140–149, Jul. 2017.
[16] Y. Yu, S. Gao, Y. Wang, and Y. Todo, "Global optimum-based search differential evolution," *IEEE/CAA J. Autom. Sinica*, vol. 6, no. 2, pp. 379–394, Mar. 2019.
[17] S. Gao, Y. Yu, Y. Wang, J. Wang, J. Cheng, and M. Zhou, "Chaotic local search-based differential evolution algorithms for optimization," *IEEE Trans. Syst., Man, Cybern., Syst.*, to be published, doi: 10.1109/tsmc.2019.2956121.
[18] P. J. Van Laarhoven and E. H. Aarts, "Simulated annealing," in *Simulated Annealing: Theory and Applications*. Dordrecht, The Netherlands: Springer, 1987, pp. 7–15.
[19] E. Rashedi, H. Nezamabadi-Pour, and S. Saryazdi, "GSA: A gravitational search algorithm," *Inf. Sci.*, vol. 179, no. 13, pp. 2232–2248, Jun. 2009.
[20] F. Glover and M. Laguna, "Tabu search," in *Handbook of Combinatorial Optimization*. Boston, MA, USA: Springer, 1998, pp. 2093–2229.
[21] E. Atashpaz-Gargari and C. Lucas, "Imperialist competitive algorithm: An algorithm for optimization inspired by imperialistic competition," in *Proc. IEEE Congr. Evol. Comput.*, Sep. 2007, pp. 4661–4667.
[22] E. Rashedi, E. Rashedi, and H. Nezamabadi-Pour, "A comprehensive survey on gravitational search algorithm," *Swarm Evol. Comput.*, vol. 41, pp. 141–158, Aug. 2018.
[23] S. Sarafrazi, H. Nezamabadi-Pour, and S. Saryazdi, "Disruption: A new operator in gravitational search algorithm," *Sci. Iranica*, vol. 18, no. 3, pp. 539–548, Jun. 2011.
[24] H. Nobahari, M. Nikusokhan, and P. Siarry, "A multi-objective gravitational search algorithm based on non-dominated sorting," *Int. J. Swarm Intell. Res.*, vol. 3, no. 3, pp. 32–49, Jul. 2012.
[25] M. Khatibinia and S. Khosravi, "A hybrid approach based on an improved gravitational search algorithm and orthogonal crossover for optimal shape design of concrete gravity dams," *Appl. Soft Comput.*, vol. 16, pp. 223–233, Mar. 2014.
[26] P. Haghbayan, H. Nezamabadi-Pour, and S. Kamyab, "A niche GSA method with nearest neighbor scheme for multimodal optimization," *Swarm Evol. Comput.*, vol. 35, pp. 78–92, Aug. 2017.
[27] S. Gao, C. Vairappan, Y. Wang, Q. Cao, and Z. Tang, "Gravitational search algorithm combined with chaos for unconstrained numerical optimization," *Appl. Math. Comput.*, vol. 231, pp. 48–62, Mar. 2014.
[28] S. Sarafrazi, H. Nezamabadi-Pour, and S. R. Seydnejad, "A novel hybrid algorithm of GSA with Kepler algorithm for numerical optimization," *J. King Saud Univ.-Comput. Inf. Sci.*, vol. 27, no. 3, pp. 288–296, Jul. 2015.
[29] U. Güvenc and F. Katırcıoğlu, "Escape velocity: A new operator for gravitational search algorithm," *Neural Comput. Appl.*, vol. 31, no. 1, pp. 27–42, Jan. 2019.
[30] S. He, L. Zhu, L. Wang, L. Yu, and C. Yao, "A modified gravitational search algorithm for function optimization," *IEEE Access*, vol. 7, pp. 5984–5993, 2019.
[31] M. R. Narimani, R. Azizipanah-Abarghooee, M. Javidsharifi, and A. A. Vahed, "Enhanced gravitational search algorithm for multi-objective distribution feeder reconfiguration considering reliability, loss and operational cost," *IET Gener., Transmiss. Distrib.*, vol. 8, no. 1, pp. 55–69, Jan. 2014.
[32] G. Sun, P. Ma, J. Ren, A. Zhang, and X. Jia, "A stability constrained adaptive alpha for gravitational search algorithm," *Knowl.-Based Syst.*, vol. 139, pp. 200–213, Jan. 2018.
[33] D. Pelusi, R. Mascella, L. Tallini, J. Nayak, B. Naik, and Y. Deng, "Improving exploration and exploitation via a hyperbolic gravitational search algorithm," *Knowl.-Based Syst.*, Dec. 2019, Art. no. 105404, doi: 10.1016/j.knosys.2019.105404.
[34] S. Mirjalili and A. H. Gandomi, "Chaotic gravitational constants for the gravitational search algorithm," *Appl. Soft Comput.*, vol. 53, pp. 407–419, Apr. 2017.
[35] Z. Song, S. Gao, Y. Yu, J. Sun, and Y. Todo, "Multiple chaos embedded gravitational search algorithm," *IEICE Trans. Inf. Syst.*, vol. E100.D, no. 4, pp. 888–900, 2017.
[36] S. Mirjalili and S. Z. M. Hashim, "A new hybrid PSOGSA algorithm for function optimization," in *Proc. Int. Conf. Comput. Inf. Appl.*, Dec. 2010, pp. 374–377.
[37] A. A. Nagra, F. Han, Q.-H. Ling, and S. Mehta, "An improved hybrid method combining gravitational search algorithm with dynamic multi swarm particle swarm optimization," *IEEE Access*, vol. 7, pp. 50388–50399, 2019.
[38] B. Shaw, V. Mukherjee, and S. Ghoshal, "Solution of reactive power dispatch of power systems by an opposition-based gravitational search algorithm," *Int. J. Elect. Power Energy Syst.*, vol. 55, pp. 29–40, Feb. 2014.
[39] M. Soleimanpour-Moghadam, H. Nezamabadi-Pour, and M. M. Farsangi, "A quantum inspired gravitational search algorithm for numerical function optimization," *Inf. Sci.*, vol. 267, pp. 83–100, May 2014.
[40] Y. Wang, Y. Yu, S. Gao, H. Pan, and G. Yang, "A hierarchical gravitational search algorithm with an effective gravitational constant," *Swarm Evol. Comput.*, vol. 46, pp. 118–139, May 2019.

[41] S. özyön, C. Yaşar, and H. Temurtaş, "Incremental gravitational search algorithm for high-dimensional benchmark functions," *Neural Comput. Appl.*, vol. 31, no. 8, pp. 3779–3803, Aug. 2019.
[42] D. Pelusi, R. Mascella, L. Tallini, J. Nayak, B. Naik, and A. Abraham, "Neural network and fuzzy system for the tuning of gravitational search algorithm parameters," *Expert Syst. Appl.*, vol. 102, pp. 234–244, Jul. 2018.
[43] D. Pelusi, R. Mascella, and L. Tallini, "Revised gravitational search algorithms based on evolutionary-fuzzy systems," *Algorithms*, vol. 10, no. 2, p. 44, Apr. 2017.
[44] R. García-Ródenas, L. J. Linares, and J. A. López-Gómez, "A memetic chaotic gravitational search algorithm for unconstrained global optimization problems," *Appl. Soft Comput.*, vol. 79, pp. 14–29, Jun. 2019.
[45] H. Zandevakili, E. Rashedi, and A. Mahani, "Gravitational search algorithm with both attractive and repulsive forces," *Soft Comput.*, vol. 23, no. 3, pp. 783–825, Feb. 2019.
[46] K. Pal, C. Saha, S. Das, and C. A. C. Coello, "Dynamic constrained optimization with offspring repair based gravitational search algorithm," in *Proc. IEEE Congr. Evol. Comput.*, Jun. 2013, pp. 2414–2421.
[47] E. Rashedi, H. Nezamabadi-Pour, and S. Saryazdi, "BGSA: Binary gravitational search algorithm," *Natural Comput.*, vol. 9, no. 3, pp. 727–745, Sep. 2010.
[48] S. Gao, Y. Todo, T. Gong, G. Yang, and Z. Tang, "Graph planarization problem optimization based on triple-valued gravitational search algorithm," *IEEJ Trans. Elect. Electron. Eng.*, vol. 9, no. 1, pp. 39–48, Jan. 2014.
[49] H. Sajedi and S. F. Razavi, "DGSA: Discrete gravitational search algorithm for solving knapsack problem," *Oper. Res.*, vol. 17, no. 2, pp. 563–591, Jul. 2017.
[50] S. Sarafrazi and H. Nezamabadi-Pour, "Facing the classification of binary problems with a GSA-SVM hybrid system," *Math. Comput. Model.*, vol. 57, nos. 1–2, pp. 270–278, Jan. 2013.
[51] E. Rashedi, H. Nezamabadi-Pour, and S. Saryazdi, "A simultaneous feature adaptation and feature selection method for content-based image retrieval systems," *Knowl.-Based Syst.*, vol. 39, pp. 85–94, Feb. 2013.
[52] A. Ghosh, S. Banerjee, M. K. Sarkar, and P. Dutta, "Design and implementation of type-II and type-III controller for DC–DC switched-mode boost converter by using K-factor approach and optimisation techniques," *IET Power Electron.*, vol. 9, no. 5, pp. 938–950, 2016.
[53] O. özkaraca and A. Keçebaş, "Performance analysis and optimization for maximum exergy efficiency of a geothermal power plant using gravitational search algorithm," *Energy Convers. Manage.*, vol. 185, pp. 155–168, Apr. 2019.
[54] K.-H. Lu, C.-M. Hong, and Q. Xu, "Recurrent wavelet-based Elman neural network with modified gravitational search algorithm control for integrated offshore wind and wave power generation systems," *Energy*, vol. 170, pp. 40–52, Mar. 2019.
[55] A. V. Dhumane and R. S. Prasad, "Multi-objective fractional gravitational search algorithm for energy efficient routing in IoT," *Wireless Netw.*, vol. 25, no. 1, pp. 399–413, Jan. 2019.
[56] H. Mittal and M. Saraswat, "An automatic nuclei segmentation method using intelligent gravitational search algorithm based superpixel clustering," *Swarm Evol. Comput.*, vol. 45, pp. 15–32, Mar. 2019.
[57] H. Jia, X. Peng, W. Song, C. Lang, Z. Xing, and K. Sun, "Hybrid multiverse optimization algorithm with gravitational search algorithm for multithreshold color image segmentation," *IEEE Access*, vol. 7, pp. 44903–44927, 2019.
[58] K. Aihara and G. Matsumoto, "Forced oscillations and routes to chaos in the Hodgkin–Huxley axons and squid giant axons," in *Chaos in Biological Systems*. Boston, MA, USA: Springer, 1987, pp. 121–131.
[59] M. Falcke, R. Huerta, M. I. Rabinovich, H. D. I. Abarbanel, R. C. Elson, and A. I. Selverston, "Modeling observed chaotic oscillations in bursting neurons: The role of calcium dynamics and IP 3," *Biological*, vol. 82, no. 6, pp. 517–527, May 2000.
[60] X. Wang, "Period-doublings to chaos in a simple neural network: An analytical proof," *Complex Syst.*, vol. 5, no. 4, pp. 425–444, 1991.
[61] R. S. Lee, "Chaotic type-2 transient-fuzzy deep neuro-oscillatory network (CT2TFDNN) for worldwide financial prediction," *IEEE Trans. Fuzzy Syst.*, to be published, doi: 10.1109/TFUZZ.2019.2914642.
[62] R. Lee, "A transient-chaotic autoassociative network (TCAN) based on lee oscillators," *IEEE Trans. Neural Netw.*, vol. 15, no. 5, pp. 1228–1243, Sep. 2004.
[63] K. Chen and D. Wang, "A dynamically coupled neural oscillator network for image segmentation," *Neural Netw.*, vol. 15, no. 3, pp. 423–439, Apr. 2002.
[64] R. Lee, "IJADE surveillant—An intelligent multi-resolution composite neuro-oscillatory agent-based surveillance system," *Pattern Recognit.*, vol. 36, no. 6, pp. 1425–1444, Jun. 2003.
[65] J. D. Gibbons and S. Chakraborti, *Nonparametric Statistical Inference*. New York, NY, USA: CRC Press, 2014.
[66] S. Das and P. N. Suganthan, "Problem definitions and evaluation criteria for CEC 2011 competition on testing evolutionary algorithms on real world optimization problems," Jadavpur Univ., Kolkata, India, Tech. Rep., 2010, pp. 341–359.
[67] S. Banerjee, A. Ghosh, and N. Rana, "An improved interleaved boost converter with PSO-based optimal type-III controller," *IEEE J. Emerg. Sel. Topics Power Electron.*, vol. 5, no. 1, pp. 323–337, Mar. 2017.
[68] A. Ghosh and S. Banerjee, "Study of complex dynamics of DC–DC buck converter," *Int. J. Power Electron.*, vol. 8, no. 4, pp. 323–348, 2017.
[69] S. Banerjee, A. Ghosh, and S. Padmanaban, "Modeling and analysis of complex dynamics for dSPACE controlled closed-loop DC–DC boost converter," *Int. Trans. Elect. Energy Syst.*, vol. 29, no. 4, p. e2813, Apr. 2019.

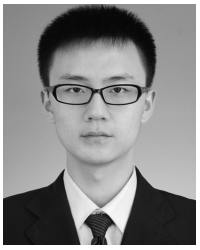

YIRUI WANG received the B.S. and M.S. degrees from the College of Information Sciences and Technology, Donghua University, Shanghai, China, in 2014 and 2017, respectively. He is currently pursuing the Ph.D. degree with the University of Toyama, Japan. His research interests are computational intelligence, swarm intelligent algorithms, and combinatorial optimizations.

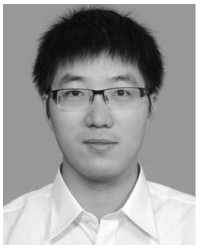

SHANGCE GAO (Senior Member, IEEE) received the Ph.D. degree in innovative life science from the University of Toyama, Toyama, Japan, in 2011.

He is currently an Associate Professor with the Faculty of Engineering, University of Toyama. His current research interests include nature-inspired technologies, mobile computing, machine learning, and neural networks for real-world applications. He was a recipient of the Best Paper Award at the IEEE International Conference on Progress in Informatics and Computing, the Shanghai Rising-Star Scientist Award, the Chen-Guang Scholar of Shanghai Award, the Outstanding Academic Performance Award of IEICE, and the Outstanding Academic Achievement Award of IPSJ. He serves as an Associate Editor for many international journals, such as IEEE Access and the IEEE/CAA Journal of Automatica Sinica. He has also served as a Secretary for Hokuriku Section, IEICE, and has served on the program committees for several international professional conferences.

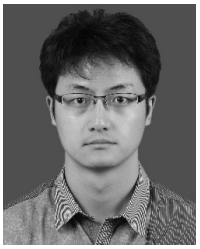

YANG YU received the B.E. degree in civil engineering from the Yancheng Institute of Technology, Yancheng, China, in 2014, and the M.S. degree from the University of Toyama, Toyama, Japan, in 2017, where he is currently pursuing the Ph.D. degree. His main research interests are data mining, optimization problems, and nature-inspired algorithms.

ZIQIAN WANG received the bachelor's degree in vehicle engineering from Hunan University, Hunan, China, in 2018. He is currently pursuing the master's degree with the University of Toyama, Toyama, Japan. His main research interests include the Internet of Vehicles and deep learning.

JIUJUN CHENG received the Ph.D. degree from the Beijing University of Posts and Telecommunications, in 2006. In 2009, he was a Visiting Professor with Aalto University, Espoo, Finland. He is currently a Professor with Tongji University, Shanghai, China. His research interests span the area of mobile computing, social network with a focus on the mobile/Internet interworking, service computing, and the Internet of Vehicles.

YUKI TODO received the B.S. degree from Zhejiang University, Zhejiang, China, in 1983, the M.S. degree from the Beijing University of Posts and Telecommunications, Beijing, China, in 1986, and the D.E. degree from Kanazawa University, Kanazawa, Japan, in 2005. From 1987 to 1989, she was an Assistant Professor with the Institute of Microelectronics, Shanghai Jiaotong University, Shanghai, China. From 1989 to 1990, she was a Research Student with Nagoya University, Nagoya, Japan. From 1990 to 2000, she was a Senior Engineer with Sanwa Newtech Inc., Miyazaki, Japan. From 2000 to 2011, she worked with the Tateyama Systems Institute, Toyama, Japan. In 2012, she joined Kanazawa University, where she is currently an Associate Professor with the Faculty of Electrical and Computer Engineering. Her current research interests include multiple-valued logic, neural networks, and optimization.